Macromolecular Research

Article

DOI 10.1007/s13233-020-8144-7

www.springer.com/13233 pISSN 1598-5032 eISSN 2092-7673

Improving Dispersion and Mechanical Properties of Polypropylene/Graphene Nanoplatelet Composites by Mixed Solvent-Assisted Melt Blending

Min Gyu Lee[1]
Sangwoon Lee[1]
Jaehyun Cho[2]
Jae Young Jho*[,1]

[1] School of Chemical and Biological Engineering, Seoul National University, Seoul 08826, Korea
[2] Institute of Advanced Composite Materials, Korea Institute of Science and Technology, Jeonbuk 54896, Korea

Received June 1, 2020 / Revised July 6, 2020 / Accepted July 8, 2020

Abstract: To improve the dispersion of graphene nanoplatelet (GNP) in polypropylene (PP), GNP was exfoliated in a mixed solvent of *p*-xylene and *N*,*N*-dimethylformamide (DMF) and the exfoliation of GNP was maintained by the addition of a compatibilizer before the melt blending. The concentration of the dispersed GNP in various ratios of the mixed solvents was measured in order to confirm the effect of the mixed solvent on the pre-treatment process. As a compatibilizer for the composite, pyrene-functionalized maleic anhydride-grafted polypropylene (Py-PP) was synthesized. The dispersion state of the composites was analyzed by the three dimensional non-destructive X-ray micro-computed tomography (3D micro-CT). The improved dispersion of GNP resulted in a significant enhancement in the mechanical properties. Young's modulus of PP composites with 2 wt% GNP has increased by 43% compared with that of PP. These results are attributed not only to the improved interfacial interaction between PP and GNP, but also to the homogeneous dispersion state of the GNP in the matrix.

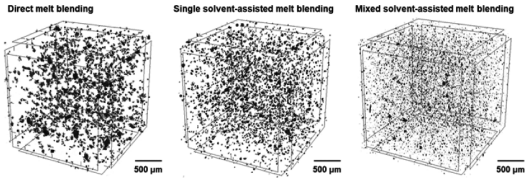

Keywords: polypropylene, graphene nanoplatelet, compatibilizer, dispersion, mechanical property.

1. Introduction

Polypropylene (PP) is one of the most important and common polyolefins due to its low cost, good processability, and recyclability. To meet the requirements for engineering applications, mechanical properties of PP need to be improved.[1] Polymer nanocomposites exhibit remarkable enhancement in electrical, thermal, and mechanical properties at low levels of filler loading compared with traditional composites.[2,3] The various allotropes of carbon such as carbon nanotube, graphene, and fullerene have been applied to improve the performance of polymer nanocomposites. As one of these carbon allotropes, graphene nanoplatelet (GNP) has attracted much attention due to its planar structure, high aspect ratio, superior Young's modulus, tensile strength, and high electrical mobility.[4,5] These properties of GNP make it a good nanofiller for polymer nanocomposites.[6]

Three main methods for fabricating polymer nanocomposites are solution blending, in situ polymerization, and melt blending. Melt blending is simple, cost-effective, and suitable for mass production in polymer manufacturing industry.[7] However, it is less effective in dispersing nanofillers than solvent-based mixing methods because of the high viscosity of molten polymers.[8,9] The dispersion state of the nanofillers and the interfacial adhesion between the filler and the polymer matrix are decisive in the mechanical properties of the polymer composite.[10-12] Thus it is necessary to improve the compatibility between nanofillers and polymer matrix during melt blending.[13,14] Several attempts using modified GNP or adding a compatibilizer have been reported for PP/GNP nanocomposites with increased mechanical properties. For modification, graphene oxide (GO) with a number of hydrophilic functional groups was used to graft alkyl or PP chains to its surface.[15-17] However, the use of GO can have reduced effect in stress transfer since the defects on GO make the sheets less stiff.[18] As a compatibilizer, chemically modified PP was added to improve the interfacial interaction between PP and GNP. For instance, PP nanocomposites compatibilized by the reacted product of maleic anhydride-grafted polypropylene (MAPP) and tryptophan showed enhanced mechanical properties.[19] The compatibilizer improved the interfacial adhesion through π-π interactions between the aromatic ring of tryptophan and GNP. Such compatibilization does not require additional modification of GNP and allows the use of GNP with less defects.

For further dispersion of nanofillers, two-step melt blending techniques with treatment of nanofillers prior to melt blending have been reported.[4] Since GNP is better exfoliated in liquid phase than in molten polymer, GNP dispersion in polymer nanocomposites can be further improved by pretreatment of GNP in an appropriate solvent. An example was reported for the PP nanocomposites fabricated by first coating GNP with PP latex in liquid phase and then melt blending it with PP matrix. The nanocomposites exhibited improved mechanical properties with well-dispersed GNP.[20] However, there is a problem in pretreatment using liquid phase for PP composites. GNP is well dispersed and exfoliated in relatively polar solvents such as *N*-methyl-2-pyrroli-

Acknowledgment: This work was supported by the Institute of Chemical Processes (ICP) at Seoul National University.

***Corresponding Author:** Jae Young Jho (jyjho@snu.ac.kr)

done and cyclopentanone, whereas a compatibilizer based on PP chain can be dissolved in non-polar solvents such as xylene.[21] It has been reported that solvent mixtures showed better dispersion of GNP in a certain ratio of the mixture than in a single solvent according to the Hansen solubility parameter (HSP) theory.[22,23]

In the present study, we applied solvent mixtures for the pretreatment of GNP in PP/GNP nanocomposites. *p*-Xylene was used to dissolve a compatibilizer based on PP chain. DMF was used because it was predicted to exfoliate GNP effectively through mixing with *p*-xylene based on the HSP theory. The *p*-xylene/DMF mixed solvent can be expected to exfoliate GNP and dissolve the compatibilizer based on PP chain without any modification of GNP or adding stabilizers. The pretreatment using such mixed solvents to achieve better GNP dispersion has not been reported in polymer nanocomposites to the best of our knowledge. Pyrene-functionalized maleic anhydride-grafted polypropylene (Py-PP) was used to prevent re-stacking of exfoliated GNP and improve the compatibility between PP and GNP. The Py-PP can be adsorbed onto GNP surface through π-π interactions and be dispersed in PP matrix due to the similar nature of MAPP and PP.[24,25] In order to find the ratio for well-dispersed GNP in the composites, we conducted pretreatment at various ratios of the mixed solvent. This work is devoted to investigating how the ratios of the pretreatment solvent affect the dispersibility and reinforcement of the PP/GNP nanocomposites through the observation of the morphology and mechanical properties.

2. Experimental

2.1. Materials

PP and maleic anhydride-grafted polypropylene (MAPP) were commercial products of Lotte Chemical with the trade name of SJ-160 and PH-200, respectively. GNP was a commercial product of XG Sciences with the trade name of xGNP-C. 1-Aminopyrene (Apy, 98%) was obtained from Tokyo Chemical Industry. *p*-Xylene (99%) and *N*,*N*-dimethylformamide (DMF, 99.5%) were purchased from Daejung Chemical.

2.2. Preparation of PP/Py-PP/GNP nanocomposites

MAPP (20 g) was dissolved in 500 mL of *p*-xylene at 120 °C for 30 min with stirring. Apy (0.6 g) was added to the solution, and stirred at 120 °C for 24 h. The product (Py-PP) was separated by precipitation in excess ethanol to remove the unreacted Apy. Py-PP was obtained after drying in a vacuum oven at 60 °C for 24 h.

A liquid-phase exfoliation method using the mixture of *p*-xylene and DMF was utilized to exfoliate GNP. The optimum ratio for dispersion of GNP was determined by examining various mixing ratios of *p*-xylene and DMF. GNP (1.0 g) was added to 500 mL of the *p*-xylene/DMF mixed solvent, and the GNP dispersion was sonicated at 60 °C for 4 h. Py-PP was added to the GNP suspension with different contents. The mixture was stirred at 120 °C for 1 h, and centrifuged at 10,000 rpm for 1 h to remove the solvent.[26-31] Py-PP/GNP was washed with ethanol and dried in a vacuum oven at 40 °C for 24 h. The PP/Py-PP/GNP composites were obtained by melt blending using an internal mixer (MKE, Rheocomp mixer 600) with the rotor speed of 100 rpm at 200 °C for 10 min. The amount of GNP was held constant at 2 wt%. The number inside the parenthesis, after the letter GNP, refers to the *p*-xylene/DMF ratio.

2.3. Characterization

The concentration of dispersed GNP in the mixed solvents was measured by a UV-Vis spectrophotometer (KLAB, Optizen Pop). The thickness of GNP which was exfoliated in the mixed solvent was identified using atomic force microscopy (AFM, Asylum Research, MFP-3D) with tapping mode. The chemical structure of Py-PP was analyzed by a Fourier transform infrared spectrometer (FT-IR, Thermo Scientific, Nicolet 6700) in attenuated total reflection mode. Morphological information about the Py-PP/GNP was obtained using an X-ray diffractometer (XRD, Bruker, D8-Advance) with a Cu Kα radiation source in the range of 2θ = 10~40°.

The fracture surface microstructure of the composites was examined using a field emission scanning electron microscopy (FE-SEM, JEOL, JSM-6701F). For the sample preparation, the specimens were frozen with liquid nitrogen for 1 min and fractured into pieces. Three dimensional non-destructive X-ray micro-computed tomography (3D micro-CT) images for dispersion state of GNP in PP matrix were scanned with a high-resolution X-ray micro-CT system (Bruker, Skyscan 1172). The composite specimens were cut into sizes of ca. 2 × 2 × 2 mm^3. Scan data were acquired with an X-ray tube setting of 23 kV and 116 μA, and the pixel size of 1.36 μm. Micro-CT images of the composites were obtained by reconstructing the projections.

The test specimens were prepared using a micro injector system (Bautek, BA-915A). The cylinder and mold temperature used were 200 °C and 25 °C, respectively. Young's modulus, tensile strength, and elongation at break were determined using a universal testing machine (UTM, Lloyds Instruments, LR10K). The tests were carried out at 25 °C with the crosshead speed of 10 mm/min and specimens of 63.0 × 3.2 × 3.1 mm^3 in dimension according to ASTM D638 type V method. The thermal stability of the composites was examined by thermo-gravimetric analysis (TGA, TA Instrument, SDT-Q600) at temperatures ranging from 100 to 600 °C at a heating rate of 10 °C/min under a nitrogen atmosphere. The crystallization and melting behaviors of the composites were carried out by differential scanning calorimetry (DSC, TA Instrument, SDT-Q600). Samples were heated from 80 to 200 °C at a rate of 10 °C/min, cooled to 80 °C, and reheated to 200 °C at the same rate under a nitrogen atmosphere.

3. Results and discussion

3.1. Dispersion of GNP in *p*-xylene/DMF mixed solvents

To determine the concentration of the dispersed GNP in the mixed solvent, the UV-Vis absorbance of the solution was investigated based on the Beer-Lambert law. The UV-vis absorbance at 660 nm is commonly used to measure the concentration of GNP dispersion.[22,23,32] Figure 1 showed the solubility parameter distance (Ra) and the dispersed concentration of GNP in the mixed sol-

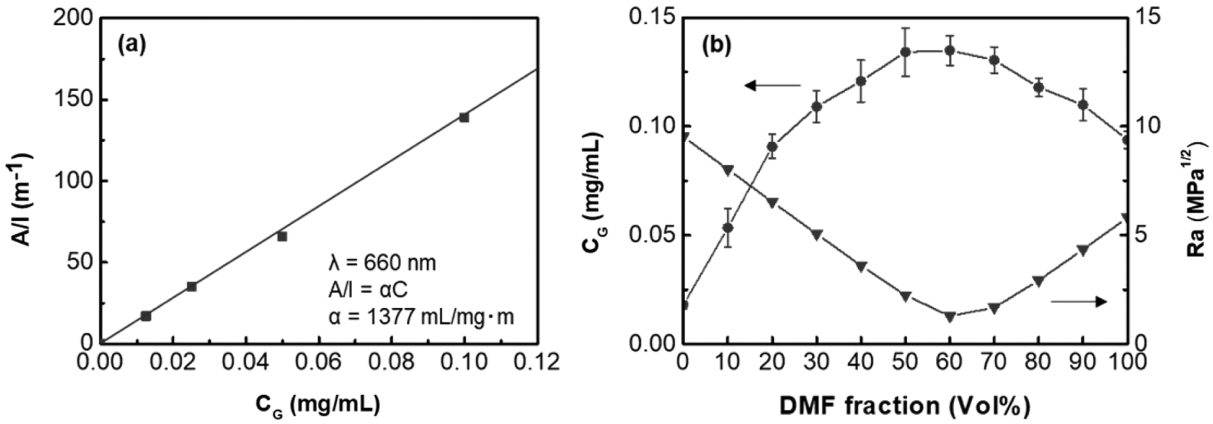

Figure 1. (a) Absorbance per unit path length (λ = 660 nm), A/l, as a function of concentration of GNP, in *p*-xylene/DMF mixtures (50 vol% DMF). Beer-Lambert behavior is shown, with an absorption coefficient (α) of 1,377 mL $mg^{-1}m^{-1}$. (b) The calculated Ra (▼) and the GNP concentration (●), as a function of the DMF volume fraction.

vents of various ratios. According to the HSP theory, the solubility parameter (δ) can be divided into δ_d, δ_p, and δ_h, which correspond to dispersive, polar, and hydrogen bond, respectively. The smaller the difference in δ_d, δ_p, and δ_h between the two substances, the better the two materials can be mixed. Ra is the distance between the parameters of two materials in the Hansen space, which can more accurately describe the affinity for each other than the use of the total or Hildebrand solubility parameter.[33] To predict the dispersibility of GNP in the mixed solvent, Ra was used here and calculated by

$$Ra = [4(\delta_{dG}-\delta_{dM})^2+(\delta_{pG}-\delta_{pM})^2+(\delta_{hG}-\delta_{hM})^2]^{1/2} \quad (1)$$

where the subscripts G and M denote GNP and the mixed solvent, respectively. The HSP values (δ_d, δ_p, δ_h) of GNP, *p*-xylene, and DMF used here were (18.0, 9.3, 7.7), (17.6, 1.0, 3.1), and (17.4, 13.7, 11.3), respectively.[21,33] The absorption coefficient α of GNP in the mixed solvent of 5 to 5 ratio was determined through the absorbance of the standard solutions. The absorbance coefficient of GNP at 660 nm was measured to be 1,377 mL mg^{-1} m^{-1}, which agreed with the reported value (Figure 1(a)).[32] As shown in Figure 1(b), after decreasing to a minimum at 60 vol% of DMF, Ra increased with further addition of DMF. This is attributed to the increase in the polar and hydrogen-bonding components of the solubility parameter. Higher concentrations of

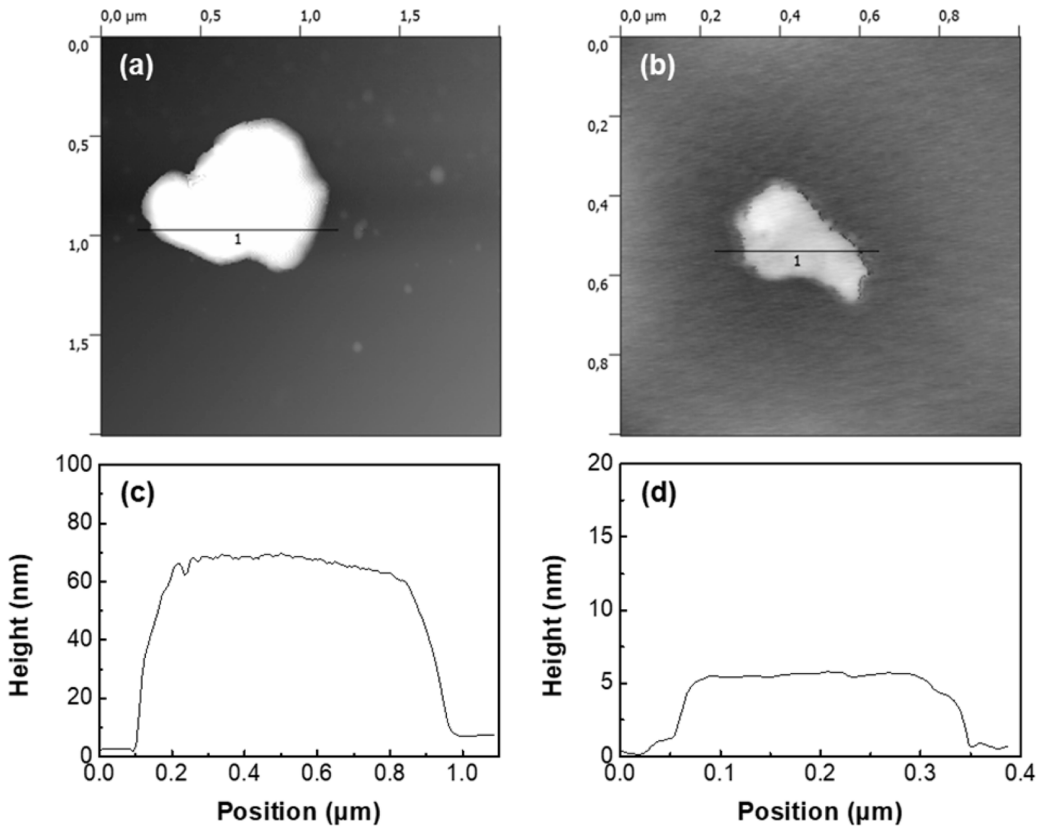

Figure 2. AFM images of (a) GNP(10/0) and (b) GNP(4/6) on a Si substrate. The height profiles of (c) GNP(10/0) and (d) GNP(4/6).

dispersed GNP were observed in the mixed solvent with smaller Ra. *p*-Xylene/DMF at the mixture ratio of 4 to 6 which had the smallest Ra with GNP showed the highest concentration of GNP.

The thickness of GNP exfoliated in a single solvent of *p*-xylene and in *p*-xylene/DMF mixed solvent of 4 to 6 ratio was identified by AFM tapping mode (Figure 2). With the same preparation steps, average thickness of GNP(10/0) and GNP(4/6) were found to be around 60 nm and 5 nm, respectively. GNP was better exfoliated in the mixed solvent than in the single solvent. The average thickness of GNP(4/6) indicated that about 5 layers of graphene were stacked.[5] This result showed a similar degree of exfoliation to that of other good solvents for GNP such as *N*-methyl-2-pyrrolidone.[21] Compared with such solvents, the mixed solvent had the advantage of dissolving the compatibilizer.

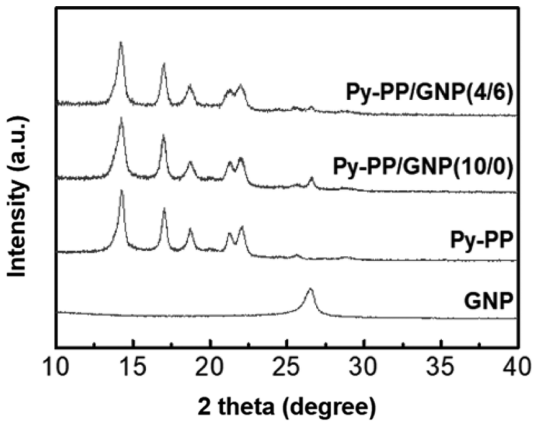

Figure 4. XRD patterns of GNP, Py-PP, Py-PP/GNP(10/0), and Py-PP/GNP(4/6).

3.2. Chemical structure of Py-PP

Py-PP was synthesized by the reaction between the maleic anhydride groups of MAPP and amine groups of Apy. The structure of the synthesized Py-PP was investigated by FT-IR analyses. Figure 3 showed the FT-IR spectra of Apy, MAPP, and Py-PP. In the spectrum of MAPP, the peaks between 2750 and 3000 cm^{-1} were attributed to the stretching of C-H bonds of polypropylene. Carbonyl stretching originating from anhydride and acid groups appeared at 1775 and 1710 cm^{-1}, respectively. The spectrum of Py-PP was similar to that of MAPP except for the characteristic peaks of Apy. The spectrum exhibited peaks at 1520, 1600, and 1623 cm^{-1} due to the stretching of aromatic C=C bonds of pyrene groups. In addition, the peak at 1410 cm^{-1} could be assigned to the stretching vibration of C-N and the peak at 1710 cm^{-1} increased due to the reaction. The same results were observed for the reaction between maleic anhydride groups of MAPP and amine groups of aniline.[34-36] This structure of Py-PP could be utilized to both prevent the re-stacking of the exfoliated GNP and improve the interfacial interaction between PP and GNP through π-π interactions between pyrene groups of Py-PP and GNP.

3.3. Effect of mixed solvent on Py-PP/GNP structure and composite morphology

The exfoliation state of GNP was detected by using XRD analysis. The XRD patterns of GNP, Py-PP, Py-PP/GNP(10/0), and Py-PP/GNP(4/6) were given in Figure 4. Py-PP showed diffraction peaks of the crystalline phases of PP at 2θ = 14.2° (110), 17.0° (040), 18.7° (130), 21.2° (111), and 22.0° (131/041).[16] It was observed that pristine GNP showed a peak at 2θ = 26.6°, corresponding to the *d*-spacing of 0.347 nm. Py-PP/GNP(10/0) also showed a peak at 2θ = 26.6° because the GNP still remained in aggregated form as it was not exfoliated effectively in the single solvent. In contrast, Py-PP/GNP(4/6) did not show a peak at 2θ = 26.6°, implying that re-stacking of the exfoliated GNP was prevented.[24] This exfoliated state of GNP led to good dispersion of the filler during the melt blending.

To observe the overall dispersion state of GNP in the PP matrix, Three-dimensional (3D) X-ray micro-CT analysis was conducted. 3D micro-CT analysis can investigate the internal structure of polymer nanocomposites without destroying the specimens.[24,37] Figure 5 showed 3D micro-CT images of the composites filled with 2 wt% GNP. The observed dimension of the composites was 2 × 2 × 2 mm^3. It was worthy to note that the aggregation of filler was more prominent in PP/GNP than in PP/Py-PP/GNP(10/0) and PP/Py-PP/GNP(4/6). This demonstrated that direct melt blending method was less effective in dispersing GNP and showed the necessity of additional treatments. In addition, PP/Py-PP/GNP(4/6) showed the most homogeneous dispersion of GNP, which proved that the dispersibility of GNP depended on the ratio of the mixed solvent used in the pretreatment.

In order to obtain explicit information on the morphology of the GNP inside the PP matrix, the fracture surfaces of PP/GNP

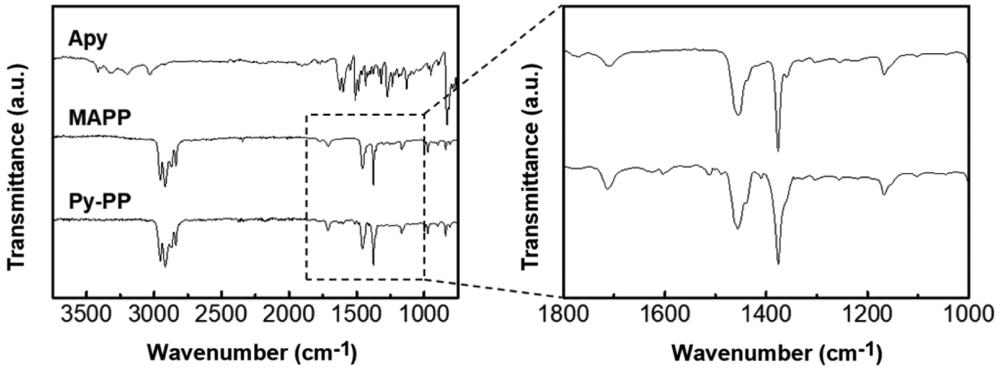

Figure 3. FT-IR spectra of Apy, MAPP, and Py-PP.

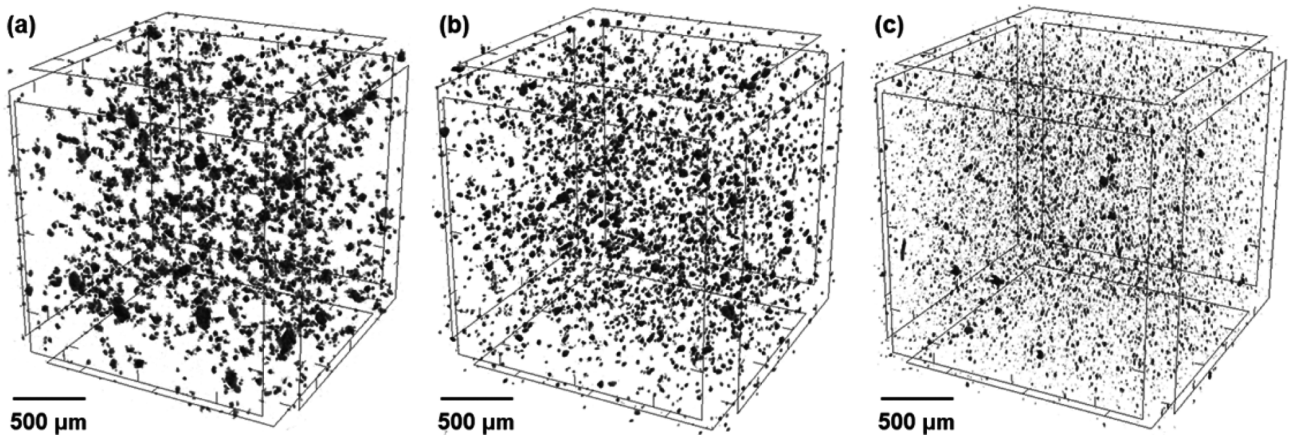

Figure 5. 3D micro-CT images of (a) PP/GNP, (b) PP/Py-PP/GNP(10/0), and (c) PP/Py-PP/GNP(4/6).

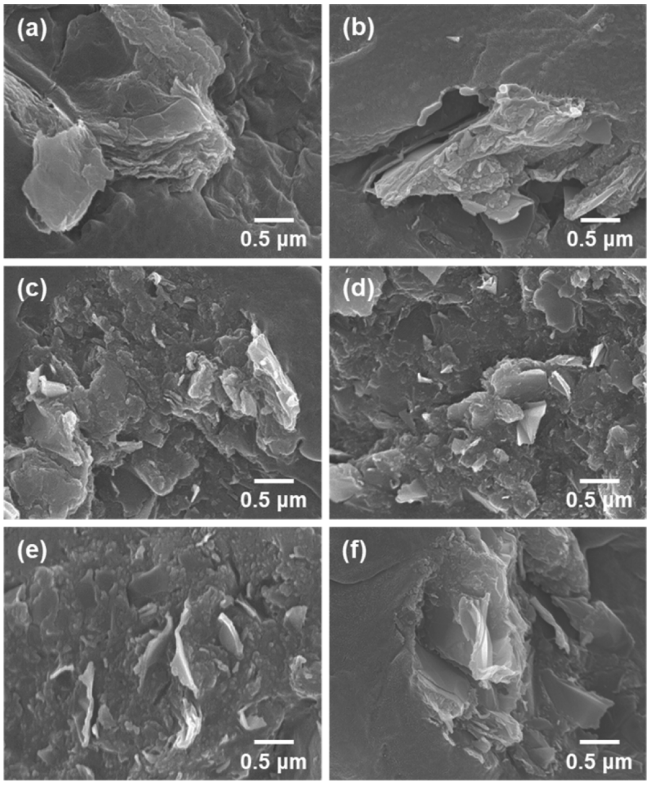

Figure 6. SEM micrographs of the cryofracture surface of (a) PP/GNP and PP/Py-PP/GNP composites with various mixing ratios of the *p*-xylene/DMF ysolvents: (b) 10/0, (c) 8/2, (d) 6/4, (e) 4/6, and (f) 0/10.

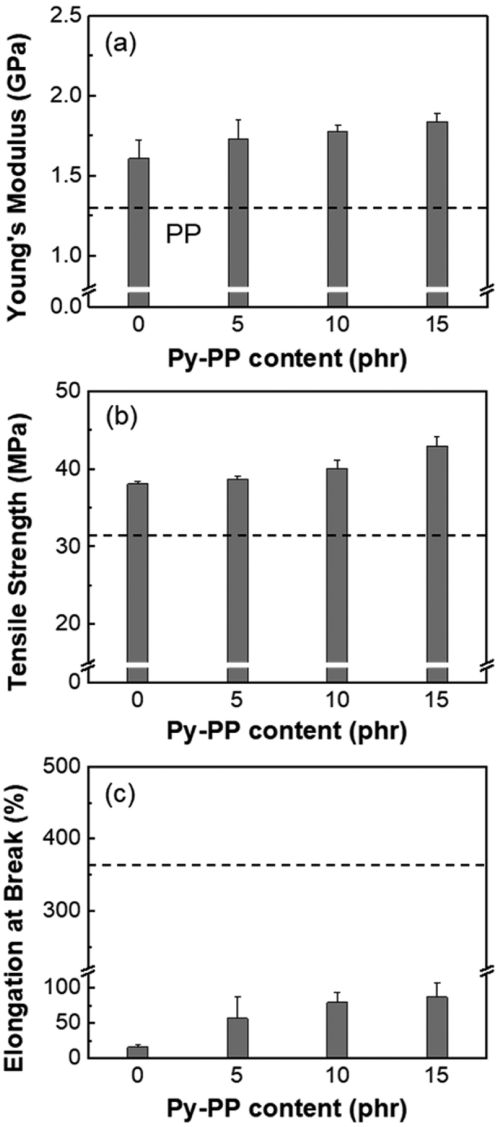

Figure 7. Measurements of mechanical properties: (a) Young's modulus, (b) tensile strength, and (c) elongation at break of PP/Py-PP/GNP(4/6) composites as a function of the compatibilizer content.

and PP/Py-PP/GNP composites were examined. SEM images shown in Figure 6 revealed the difference in size and the degree of exfoliation of GNP. Large and aggregated forms of GNP were observed in PP/GNP due to the poor interfacial interaction between the composite components during the melt blending. The addition of Py-PP/GNP(10/0) led to reduction in size of GNP by increasing interfacial interaction but the GNP was still in stacked form. GNP showed improved dispersion in the composites as the volume fraction of DMF in the pretreatment solvent increased. GNP was exfoliated the most in the composite blended with Py-PP/GNP(4/6) due to the effects of the mixed solvent and the compatibilizer. However, the GNP in PP/Py-PP/GNP(0/10) composite showed stacked forms similar with GNP in PP/Py-PP/GNP(10/0) because the pretreatment solvent was not able to dissolve the compati-

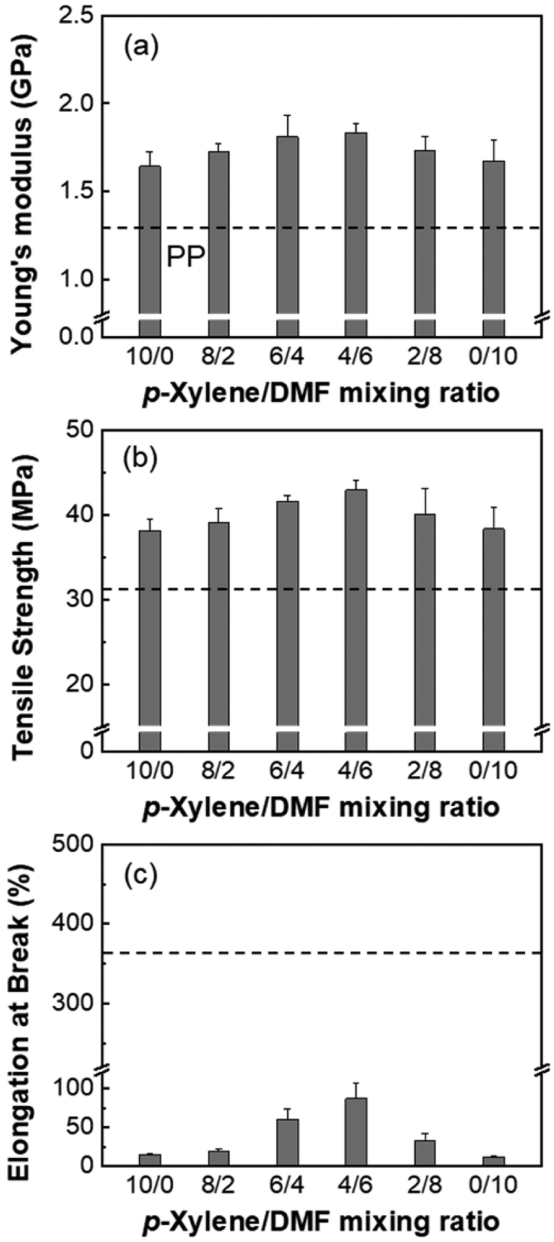

Figure 8. Measurements of mechanical properties: (a) Young's modulus, (b) tensile strength, and (c) elongation at break of PP/Py-PP/GNP composites with various mixing ratios of the solvents.

blizer, causing re-aggregation of GNP. It was noteworthy that the pretreatment solvent should not only exfoliate GNP but also dissolve the compatibilizer for prevention of GNP re-stacking.

3.4. Mechanical properties and thermal behaviors of PP/Py-PP/GNP composites

Figure 7 showed the tensile properties of PP/Py-PP/GNP(4/6) composites according to the content of the compatiblizer. The filler loading was fixed at 2 wt%. As the content of Py-PP increased, the Young's modulus and tensile strength of the composites increased. The effective stress transferring to exfoliated GNP occurred because the interfacial adhesion improved with increasing amount of the compatibilizer. A similar result was reported for PP/GNP nanocomposites fabricated with MAPP as a compatibilizer. The result showed enhanced mechanical properties with increasing amount of MAPP.[38] The elongation at break of PP/GNP dramatically decreased compared with that of PP, which is a typical brittle fracture behavior of composites with rigid fillers due to the poor interfacial adhesion and defects between the matrix and the filler.[24] On the other hand, all of the composites added with Py-PP/GNP(4/6) showed higher elongation at break as the interface was stable.

In order to confirm the effect of the mixed solvent on the mechanical properties of the PP composites, the tensile properties of composites pretreated with the solvents of various mixing ratios were investigated (Figure 8). The composites were filled with 2 wt% GNP and 15 phr Py-PP. The Young's modulus and tensile strength of PP/Py-PP/GNP(10/0) increased compared with those of PP. The elongation at break of PP/Py-PP/GNP(10/0) showed brittle fracture behavior because defects existing in the interface between the matrix and the stacked GNP acted as stress concentrators.[39] The composites pretreated with mixed solvents showed higher tensile properties than PP/Py-PP/GNP (10/0). When the ratio of *p*-xylene to DMF was 4 to 6, the Young's modulus and tensile strength were the highest, which were 41% and 34% higher than those of PP, respectively. This was the result of the stress transfer improving with higher aspect ratio of exfoliated GNP.[40-44] In addition, the nanoscale fillers restricted the polymer chain mobility at the interface, increasing the stiffness of the composites.[45] The composites pretreated by the mixed

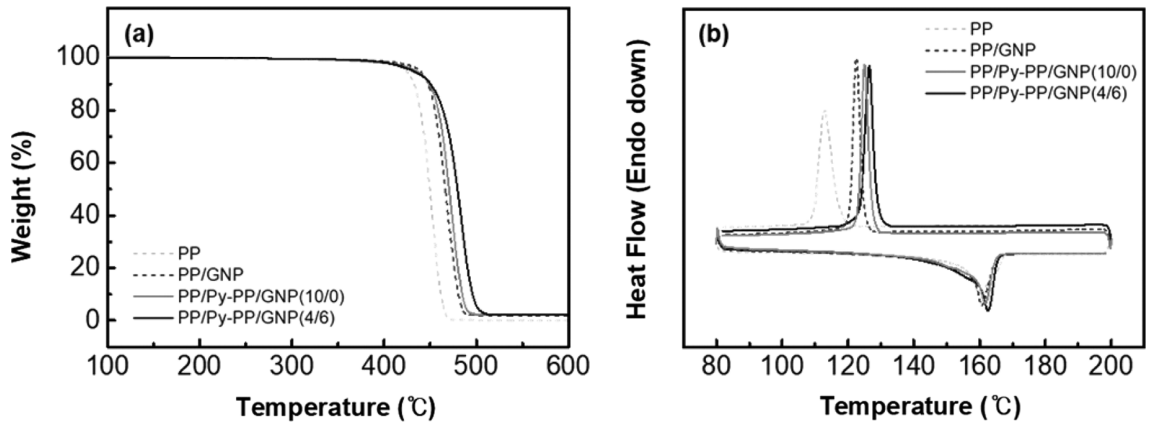

Figure 9. (a) TGA and (b) DSC data of PP, PP/GNP, PP/Py-PP/GNP(10/0), and PP/Py-PP/GNP(4/6).

Table 1. Crystallization temperature (T_c), melting temperature (T_m), and degree of crystallinity (X_c) of PP, PP/GNP, PP/Py-PP/GNP(10/0), and PP/Py-PP/GNP(4/6)

Samples	T_c (°C)	T_m (°C)	X_c (%)
PP	112.9	160.1	46.8
PP/GNP	122.5	160.7	49.1
PP/Py-PP/GNP(10/0)	125.0	161.8	52.6
PP/Py-PP/GNP(4/6)	126.4	162.5	55.2

solvents with over 60 vol% of DMF showed gradual decrease in the tensile properties. This is because re-stacking of the GNP occurred as it became harder to dissolve Py-PP in the pretreatment step.

Figure 9(a) showed the weight loss curves of PP, PP/GNP, PP/Py-PP/GNP(10/0), and PP/Py-PP/GNP(4/6) composites at the heating rate of 10 °C/min. The temperatures for 5% weight loss ($T_{5\%}$) of PP, PP/GNP, PP/Py-PP/GNP(10/0), and PP/Py-PP/GNP(4/6) were 424, 439, 434, and 431 °C, respectively. The composites showed enhanced thermal stability at the initial stage of degradation compared with PP because GNP act as heat sink that do not allow the accumulation of heat PP. The temperatures at which there is no more thermal degradation (T_{end}) of PP, PP/GNP, PP/Py-PP/GNP(10/0), and PP/Py-PP/GNP(4/6) were 475, 494, 501, and 516 °C, respectively. The difference between T_{end} and $T_{5\%}$ of PP/Py-PP/GNP(4/6) was larger than that of PP/Py-PP/GNP(10/0), which means the improvement of the resistance to thermal degradation. This is because GNP also serve as transfer barrier and GNP with the improved dispersion more effectively hindered the volatile decomposed products.[4] DSC curves for the crystallization and melting behaviors of PP, PP/GNP, PP/Py-PP/GNP(10/0), and PP/Py-PP/GNP(4/6) composites were shown in Figure 9(b). Table 1 showed the crystallization temperature (T_c), melting temperature (T_m), and degree of crystallinity (X_c) of the specimens. Due to the effect of heterogeneous nucleating agent of GNP, the composites crystallize at a higher temperature than PP. PP/Py-PP/GNP(4/6) composite showed the highest T_c and X_c because the improved dispersion of GNP caused an increase in heterogeneous nucleating sites and induced crystallization of PP matrix.[46,47]

4. Conclusions

PP/GNP nanocomposites were fabricated by the melt blending assisted with *p*-xylene/DMF mixed solvent. Py-PP, which was synthesized by reacting MAPP with Apy, was used to prevent re-stacking of exfoliated GNP in the mixed solvents and as a compatibilizer between PP and GNP. *p*-Xylene/DMF mixed solvents with various ratios were investigated for the pretreatment of GNP. Adding Py-PP prevented re-stacking of exfoliated GNP through π-π interactions during the drying process. By obtaining SEM and 3D micro-CT images, the extent of the exfoliation and dispersion of GNP in the composites were directly monitored. While GNP was still in stacked form in the composite when only *p*-xylene was used, the exfoliation and dispersion of GNP were improved in the composites when the mixed solvents were used. As the DMF volume fraction of the mixed solvent increased, the exfoliation of GNP was improved, and prominent dispersion at 4 to 6 ratio was observed. Comparing the mechanical properties of the composites, the Young's modulus and tensile strength increased by adding Py-PP and treating GNP in the mixed solvent. The ratio of the most effective mixed solvent for GNP dispersion was established, and Young's modulus and elongation at break were greatly enhanced in the PP/Py-PP/GNP(4/6) composite due to the improved dispersion of GNP and interfacial adhesion between the matrix and the fillers. It was certain that the melt blending assisted with the mixed solvent was more effective in dispersing GNP than the direct melt blending.

References

(1) S. N. Tripathi, G. S. S. Rao, A. B. Mathur, and R. Jasra, *RSC Adv.*, **7**, 23615 (2017).
(2) W. K. Chee, H. N. Lim, N. M. Huang, and I. Harrison, *RSC Adv.*, **5**, 68014 (2015).
(3) Q. Lu, H. S. Jang, W. J. Han, J. H. Lee, and H. K. Choi, *Macromol. Res.*, **27**, 1061 (2019).
(4) B. Li and W.-H. Zhong, *J. Mater. Sci.*, **46**, 5595 (2011).
(5) M. J. Allen, V. C. Tung, and R. B. Kaner, *Chem. Rev.*, **110**, 132 (2010).
(6) H. Kim, A. A. Abdala, and C. W. Macosko, *Macromolecules*, **43**, 6515 (2010).
(7) T. Kuilla, S. Bhadra, D. Yao, N. H. Kim, S. Bose, and J. H. Lee, *Prog. Polym. Sci.*, **35**, 1350 (2010).
(8) G. Mittal, V. Dhand, K. Y. Rhee, S.-J. Park, and W. R. Lee, *J. Ind. Eng. Chem.*, **21**, 11 (2015).
(9) K. Kalaitzidou, H. Fukushima, and L. T. Drzal, *Compos. Sci. Technol.*, **67**, 2045 (2007).
(10) D. R. Paul and L. M. Robeson, *Polymer*, **49**, 3187 (2008).
(11) H. Kwon, D. Kim, J. Seo, and H. Han, *Macromol. Res.*, **21**, 987 (2013).
(12) D. G. Papageorgiou, I. A. Kinloch, and R. J. Young, *Prog. Mater. Sci.*, **90**, 75 (2017).
(13) K. H. Jung, H. J. Kim, M. H. Kim, and J.-C. Lee, *Macromol. Res.*, **28**, 241 (2020)
(14) S. Ganguly, S. Mondal, P. Das, P. Bhawal, T. K. Das, S. Chosh, S. Ramanan, and N. C. Das, *Macromol. Res.*, **27**, 268 (2019).
(15) J.-H. Woo and S.-Y. Park, *Macromol. Res.*, **24**, 508 (2016).
(16) S. H. Ryu and A. M. Shanmugharaj, *Mater. Chem. Phys.*, **146**, 478 (2014).
(17) N. Song, J. Yang, P. Ding, S. Tang, Y. Liu, and L. Shi, *Ind. Eng. Chem. Res.*, **53**, 19951 (2014).
(18) O. C. Compton and S. T. Nguyen, *Small*, **6**, 711 (2010).
(19) F. You, D. Wang, X. Li, M. Liu, G.-H. Hu, and Z.-M. Dang, *RSC Adv.*, **4**, 8799 (2014).
(20) P. Song, Z. Cao, Y. Cai, L. Zhao, Z. Fang, and S. Fu, *Polymer*, **52**, 4001 (2011).
(21) Y. Hernandez, M. Lotya, D. Rickard, S. D. Bergin, and J. N. Coleman, *Langmuir*, **26**, 3208 (2010).
(22) W.-W. Liu, B.-Y. Xia, X.-X. Wang, and J.-N. Wang, *Front. Mater. Sci.*, **6**, 176 (2012).
(23) M. Yi, Z. Shen, X. Zhang, and S. Ma, *J. Phys. D: Appl. Phys.*, **46**, 025301 (2013).
(24) J. Cho, I. Jeon, S. Y. Kim, S. Lim, and J. Y. Jho, *ACS Appl. Mater. Interfaces*, **9**, 27984 (2017).
(25) D. Parviz, S. Das, H. S. T. Ahmed, F. Irin, S. Bhattacharia, and M. J. Green, *ACS Nano*, **6**, 8857 (2012).
(26) D. Dastan, *Appl. Phys. A*, **123**, 299 (2017).
(27) W.-D. Zhou, D. Dastan, J. Li, X.-T. Yin, and Q. Wang, *Nanomaterials*, **10**, 785 (2020)
(28) X.-T. Yin, J. Li, D. Dastan, W.-D. Zhou, H. Garmestani, and F. M. Alamgir, *Sens. Actuators B*, **319**, 128330 (2020).

(29) D. Dastan and A. Banpurkar, *J. Mater. Sci.*, **28**, 3851 (2017).
(30) D. Dastan, P. U. Londhe, and N. B. Chaure, *J. Mater. Sci.*, **25**, 3473 (2014).
(31) X.-T. Yin, W.-D. Zhou, J. Li, P. Lv, Q. Wang, D. Wang, F. Wu, D. Dastan, H. Garmestani, Z. Shi, and S. Talu, *J. Mater. Sci.*, **30**, 14687 (2014).
(32) M. Lotya, Y. Hernandez, P. J. King, R. J. Smith, V. Nicolosi, L. S. Karlsson, F. M. Blighe, S. De, Z. Wang, I. T. McGovrn, G. S. Duesberg, and J. N. Coleman, *J. Am. Chem. Soc.*, **131**, 3611 (2009).
(33) C. M. Hansen, *Solubility Parameters–An Introduction,* in *Hansen Solubility Parameter: A User's Handbook*, CRC Press, Boca Raton, 2000.
(34) J. G. Martínez-Colunga, S. Sanchez-Valdes, L. F. Ramos-deValle, O. Perez-Camacho, E. Ramirez-Vargas, R. Benavides-Cantú, C. A. Avila-Orta, V. J. Cruz-Delgado, J. M. Mata-Padilla, T. Lozano-Ramírez, and A. B. Espinoza-Martínez, *Polym.-Plast. Technol. Eng.*, **57**, 1360 (2017).
(35) W. Hu, T. Li, D. Dastan, K. Ji, and P. Zhao, *J. Alloy. Comp.*, **818**, 152933 (2020).
(36) D. Dastan, S. L. Panahi, and N. B. Chaure, *J. Mater. Sci.*, **27**, 12291 (2016).
(37) J. You, H.-H. Choi, Y. M. Lee, J. Cho, M. Park, S.-S. Lee, and J. H. Park, *Compos. Part B: Eng.*, **164**, 710 (2019).
(38) J. U. Roh, S. W. Ma, W. I. Lee, H. Thomas Hahn, and D. W. Lee, *Compos. Part B: Eng.*, **45**, 1548 (2013).
(39) A. J. Duguay, J. W. Nader, A. Kiziltas, D. J. Gardner, and H. J. Dagher, *Appl. Nanosci.*, **4**, 279 (2013).
(40) L. Gong, I. A. Kinloch, R. J. Young, I. Riaz, R. Jalil, and K. S. Novoselov, *Adv. Mater.*, **22**, 2694 (2010).
(41) S. R. Ahmad, C. Xue, and R. J. Young, *Mater. Sci. Eng. B*, **216**, 2 (2017).
(42) J. T. Choi, D. H. Kim, K. S. Ryu, H. M. Jeong, C. M. Shin, J. H. Kim, and B. K. Kim, *Macromol. Res.*, **19**, 809 (2011).
(43) L. Liu, Y. Sheng, M. Liu, M. Dienwiebel, Z. Zhang, and D. Dastan, *Tribol. Int.*, **140**, 105727 (2019).
(44) M. Liu, C. Y. Li, L. Liu, Y. Ye, D. Dastan, and H. Garmestani, *Mater. Sci. Technol.*, **36**, 284 (2020).
(45) X. L. Ji, J. K. Jing, W. Jing, and B. Z. Jiang, *Polym. Eng. Sci.*, **42**, 983 (2002).
(46) J.-Z. Xu, C. Chen, Y. Wang, H. Tang, Z.-M. Li, and B. S. Hsiao, *Macromolecules*, **44**, 2808 (2011).
(47) M. Mucha, J. Marszalek, and A. Fidrych, *Polymer*, **41**, 4137 (2000).

